ISSN 1330-3651 (Print), ISSN 1848-6339 (Online)
Received: 10 July 2025; Accepted: 14 January 2026

https://doi.org/10.17559/TV-20250710002814
Original scientific paper

Backstepping Sliding Mode Controller Design for Series DC Motor Control under Parameter Uncertainty and Disturbance

Hamed Khaled SHREITEH, Hilmi AYGÜN*

Abstract: Series DC motors are commonly used in applications such as elevators, cranes, and electric trains due to their high starting torque. However, their nonlinear characteristics make conventional PID controllers inadequate, particularly in handling parameter uncertainties and external disturbances. Furthermore, improper tuning of PID parameters can lead to system instability. To address these challenges and improve both transient and dynamic performance, this paper proposes a backstepping sliding mode controller. The proposed method combines the advantages of backstepping and sliding mode control, ensuring robust performance and system stability through Lyapunov-based analysis. The controller's effectiveness is evaluated through MATLAB simulations under scenarios involving sudden speed changes, load disturbances, and ±50% parameter uncertainty. Comparative results demonstrate that the proposed controller outperforms conventional backstepping and sliding mode controllers, offering superior robustness and dynamic response.

Keywords: backstepping control; backstepping sliding mode control; nonlinear control; series DC motor; sliding mode control

1 INTRODUCTION

Due to the series connection of the field and armature windings in a series DC motor, the torque produced is proportional to the square of the armature current. This characteristic allows the motor to deliver high torque per ampere compared to other types of DC motors [1]. As a result, series DC motors are widely used in applications that demand high starting torque at low speeds, such as underground trains, elevators, milling machines, and electric vehicles [2, 11]. However, their nonlinear and load-dependent dynamic behavior poses significant challenges for precise speed regulation. These motors tend to run slowly under heavy loads and very quickly under light loads, making consistent control difficult under varying operating conditions [14].

Although a wide range of control strategies has been proposed for series DC motor speed regulation, many existing approaches exhibit inherent limitations when confronted with the motor's strongly nonlinear, load-dependent, and uncertain dynamics.

Classical linear controllers such as PI and PID remain the most commonly adopted solutions due to their simplicity and ease of implementation. Studies such as [3-6] demonstrate that acceptable speed regulation can be achieved under nominal operating conditions. However, these controllers fundamentally rely on linearized motor models, which only approximate system behavior around a specific operating point. As a result, their performance deteriorates significantly under wide load variations, parameter uncertainties, and magnetic saturation effects. Moreover, extensive gain tuning is often required to balance transient performance and stability, limiting their adaptability in real-time applications.

Intelligent enhancements of PID control, including neural-network-assisted controller [7], attempt to mitigate these drawbacks by improving tuning and adaptation. While such approaches often outperform classical PID controllers in simulation and controlled experiments, they introduce additional complexity, higher computational burden, and dependence on training data quality. Furthermore, this method typically lacks rigorous stability guarantees, which restricts its applicability in safety-critical or industrial environments.

Fuzzy logic and neuro-fuzzy controllers [8-10] provide a flexible framework to handle nonlinearities and uncertainties without requiring an accurate mathematical model. However, their performance is highly sensitive to rule-base design, membership function selection, and tuning procedures, which are often subjective and problem-specific. In addition, the absence of systematic design methodologies and formal stability proofs makes it difficult to guarantee consistent performance across different operating conditions.

Other studies have utilized advanced control theory frameworks. For instance, [2] introduced a feedback linearization-based controller augmented with a linear matrix inequality (LMI) observer, where motor parameters were estimated using the Dynamic Regressor Extension and Mixing (DREM) method. In [1], an adaptive backstepping controller was designed for unknown motor parameters and external disturbances. The adaptive approach outperformed conventional backstepping by improving damping and convergence speed.

Despite these efforts, most existing methods either rely on precise modeling, which is often unrealistic under real-world uncertainties, or are vulnerable to rapid disturbances and parameter fluctuations. Furthermore, while backstepping controllers offer a systematic recursive design approach for nonlinear systems, they may lack robustness under unmodeled dynamics. Sliding mode control (SMC), on the other hand, is well known for its robustness to parameter variations and external disturbances but often suffers from chattering and complex implementation in higher-order systems.

To overcome the shortcomings such as parameter uncertainty and disturbance, this paper proposes a backstepping sliding mode controller (BSMC) for robust speed regulation of series DC motors. The proposed method combines the recursive structure, and stability guarantees of backstepping with the robustness of SMC. By integrating both strategies, the controller is capable of handling model uncertainties and external load disturbances effectively, while ensuring asymptotic stability through a Lyapunov-based framework. Although

both backstepping and SMC strategies have been individually applied to DC motor systems, their integration into a unified control framework has not yet been explored for series DC motors in the existing literature to the best of the authors' knowledge. This lack of prior application presents a gap in robust nonlinear control strategies specifically tailored to the unique dynamic characteristics of series DC motors. The present work addresses this gap by introducing a novel BSMC approach that is designed and evaluated explicitly for this motor type.

The main contributions of this paper are as follows:

1) A BSMC design is presented for the nonlinear control of series DC motors, specifically addressing ±50% parameter uncertainties and external disturbances.

2) The proposed controller is rigorously analyzed using Lyapunov stability theory to guarantee global asymptotic stability.

3) Comparative simulation studies in MATLAB demonstrate that the BSMC outperforms conventional backstepping controller and SMC in terms of speed regulation, disturbance rejection, and dynamic response.

2 SERIES DC MOTOR MODEL

The equivalent circuit of the series DC motor, illustrated in Fig. 1, shows that the armature and field windings are connected in series. Each winding is represented by a resistor and an inductor in series. As a result of this configuration, the same current flows through both windings, meaning the armature current $i_a(t)$ and the field winding current $i_f(t)$ are equal, as expressed in Eq. (1) [15].

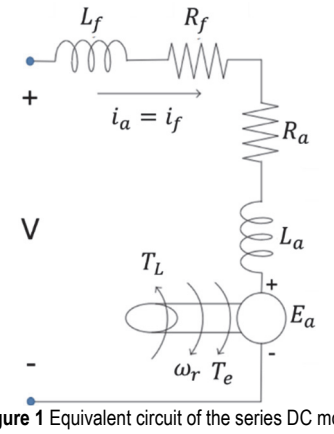

Figure 1 Equivalent circuit of the series DC motor

$$i(t) = i_a(t) = i_f(t) \tag{1}$$

The dynamic equations governing the series DC motor are as follows [12, 13]:

$$V(t) = \left(R_a + R_f\right) i(t) + \left(L_a + L_f\right) \frac{d}{dt} i(t) + E_a(t) \tag{2}$$

$$\frac{d}{dt}\omega_r(t) = \frac{1}{J}\left(T_e(t) - T_L(t) - b \cdot \omega_r(t)\right) \tag{3}$$

where $i(t)$ represents the motor current, R_a and R_f represent the armature resistance and the field winding resistance, respectively, L_a and L_f represent the armature inductance and the field winding inductance, respectively, $E_a(t)$ is the back electromotive force, $\omega_r(t)$ is the motor speed, $T_e(t)$ is the electromagnetic torque, $T_L(t)$ is the load torque, b is the viscous friction coefficient and J is the moment of inertia. The back electromotive force $E_a(t)$ and the electromagnetic torque $T_e(t)$ are given by Eq. (4) and Eq. (5), respectively.

$$E_a(t) = L_m \omega_r(t) i(t) \tag{4}$$

$$T_e(t) = L_m i(t)^2 \tag{5}$$

By defining the state variables $x_1 = \omega_r(t)$ and $x_2 = i(t)$, the series DC motor model can be formulated in state-space form as shown in Eqs. (6) and (7).

$$\dot{x}_1 = \frac{1}{J}\left(M x_2^2 - T_L - b x_1\right) \tag{6}$$

$$\dot{x}_2 = \frac{1}{L}\left(u - M x_1 x_2 - R x_2\right) \tag{7}$$

where $R = R_a + R_f$, $L = L_a + L_f$ and $M = L_m$. From Eq. (6), it is understood that the series DC motor is a nonlinear system. As seen in Eq. (6), the presence of the nonlinear term x_2^2 confirms that the series DC motor exhibits nonlinear dynamics.

3 NONLINEAR CONTROLLERS

3.1 Backstepping Controller Design

The backstepping control strategy is based on a recursive Lyapunov design framework, which systematically stabilizes the nonlinear dynamics of the systems [16, 17].

The controller design for the series DC motor proceeds in two hierarchical steps. First, the mechanical subsystem is stabilized by defining a speed tracking error and constructing a Lyapunov function to derive a virtual control law. This virtual control corresponds to the square of the armature current, which directly influences the developed electromagnetic torque. By properly selecting this virtual control, the speed tracking error is guaranteed to converge to zero.

In the second step, the electrical subsystem is incorporated into the design. An additional error variable is defined to represent the deviation between the actual armature current dynamics and the desired virtual control. A composite Lyapunov function is then formulated to include both mechanical and electrical error dynamics. The actual control input, namely the armature voltage, is derived such that the time derivative of the Lyapunov function is negative definite, ensuring global asymptotic stability of the closed-loop system.

This recursive design structure allows the nonlinearities of the series DC motor to be explicitly handled while guaranteeing stability and robustness against load torque variations.

Fig. 2 shows the block diagram of the backstepping controller. The mentioned sequential steps are implemented for speed control of a series DC motor as shown below:

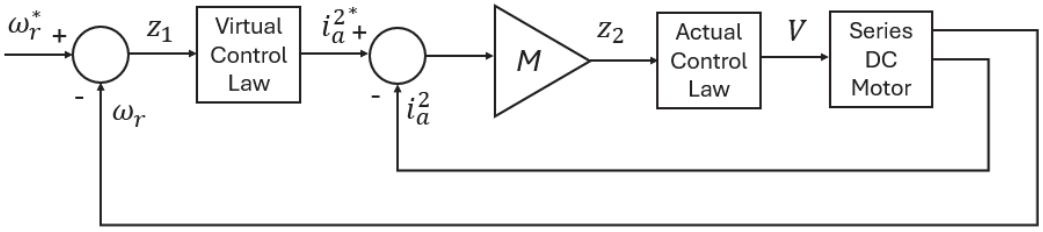

Figure 2 Block diagram of the backstepping controller

Step 1:

The speed tracking error, which needs to be compensated, is defined in Eq. (8).

$$z_1 = x_1^* - x_1 \tag{8}$$

where x_1^* denotes the reference speed. The derivative of the speed error is given by Eq. (9).

$$\dot{z}_1 = \dot{x}_1^* - \dot{x}_1 \tag{9}$$

Substituting the speed derivative $\dot{x}_1$ from Eq. (6) into Eq. (9) yields the speed error derivative as presented in Eq. (10).

$$\dot{z}_1 = \dot{x}_1^* - \frac{1}{J}\left(M\,x_2^2 - T_L - b\,x_1\right) \tag{10}$$

Eq. (11) presents the first Lyapunov function, which is used to derive the virtual control variable.

$$V_1 = \frac{1}{2}z_1^2 \tag{11}$$

The derivative of this Lyapunov function is given by Eq. (12).

$$\dot{V}_1 = z_1\dot{z}_1 = z_1\left[\dot{x}_1^* - \frac{1}{J}\left(Mx_2^2 - T_L - bx_1\right)\right] \tag{12}$$

To ensure system stability, the Lyapunov function derivative must satisfy $\dot{V}_1 \le 0$. Under this condition, $\dot{V}_1$ is expressed as in Eq. (13).

$$\dot{V}_1 = -k_1 z_1^2 \le 0 \tag{13}$$

where k_1 is positive control gain. To facilitate controller design, the virtual control variable is selected as x_2^2, and its reference value is defined by Eq. (14).

$$x_2^{2*} = \frac{1}{M}\left(J\dot{x}_1^* + T_L + bx_1 + Jk_1z_1\right) \tag{14}$$

Step 2:

At the second step of the design, the error variable z_2 is introduced as defined in Eq. (15).

$$z_2 = M\left(x_2^{2*} - x_2^2\right) = J\dot{x}_1^* + T_L + bx_1 + Jk_1z_1 - Mx_2^2 \tag{15}$$

By analyzing Eqs. (10) and (15), the relationship between $\dot{z}_1$ and z_2 is derived as shown in Eq. (16).

$$\dot{z}_1 = \frac{z_2 - Jk_1z_1}{J} \tag{16}$$

The derivative of z_2 is derived and presented in Eq. (17).

$$\dot{z}_2 = J\ddot{x}_1^* + \dot{T}_L + b\dot{x}_1 + Jk_1\dot{z}_1 - 2Mx_2\dot{x}_2 \tag{17}$$

Substituting the expressions for $\dot{x}_1$, $\dot{x}_2$, and $\dot{z}_1$ from Eqs. (6), (7), and (16), respectively, into Eq. (17), yields the formulation for $\dot{z}_2$ as shown in Eq. (18).

$$\begin{aligned}\dot{z}_2 = {} & J\ddot{x}_1^* + T_L + \frac{b}{J}\left(M\,x_2^2 - T_L - b\,x_1\right) + k_1\left(z_2 - J\,k_1z_1\right) - \\ & -2\frac{M\,x_2}{L}\left(u - M\,x_1x_2 - R\,x_2\right)\end{aligned} \tag{18}$$

Subsequently, the second Lyapunov candidate function is defined in Eq. (19) to facilitate the design of the actual control law.

$$V_2 = \frac{1}{2}z_1^2 + \frac{1}{2}z_2^2 \tag{19}$$

The derivative of this Lyapunov function is computed and shown in Eq. (20).

$$\dot{V}_2 = z_1\dot{z}_1 + z_2\dot{z}_2 = -k_1z_1^2 - k_2z_2^2 \le 0 \tag{20}$$

where k_2 is positive control gain. By substituting Eqs. (16) and (18) into Eq. (20), the control variable (DC voltage) required for the speed regulation of the series DC motor is derived, as shown in Eq. (21).

$$u = \left[A - B - 2\frac{M x_2}{L}\left(-M x_1 x_2 - R x_2\right) \right] \frac{L}{2M x_2} \tag{21}$$

where:

$$A = J \ddot{x}_1^* + \dot{T}_L + \frac{b}{J}\left(M x_2^2 - T_L - b x_1\right) + k_1\left(z_2 - J k_1 z_1\right) \tag{22}$$

$$B = -\frac{k_1 z_1^2}{z_2} - k_2 z_2 - \frac{z_1}{J z_2}\left(z_2 - J k_1 z_1\right) \tag{23}$$

3.2 Sliding Mode Controller Design

Sliding mode control (SMC) is a well-established robust control technique, effective in handling systems with model uncertainties and external disturbances [18]. It has been successfully applied to nonlinear systems such as series DC motors, where the control objective is to ensure asymptotic tracking of desired speed or torque references despite parameter variations and load disturbances. The control design follows a systematic procedure. First, the nonlinear dynamic model of the series DC motor is expressed in state-space form, where the angular speed is selected as the primary controlled output. Next, a tracking error is defined as the difference between the desired and actual motor speeds. Based on this error, a sliding surface is constructed to enforce desired second-order error dynamics.

The control law is then derived by differentiating the sliding surface. A discontinuous term is added to the control law to guarantee finite-time convergence of the system states to the sliding surface, thereby ensuring robustness against disturbances and modeling uncertainties. Fig. 3 shows the block diagram of the SMC.

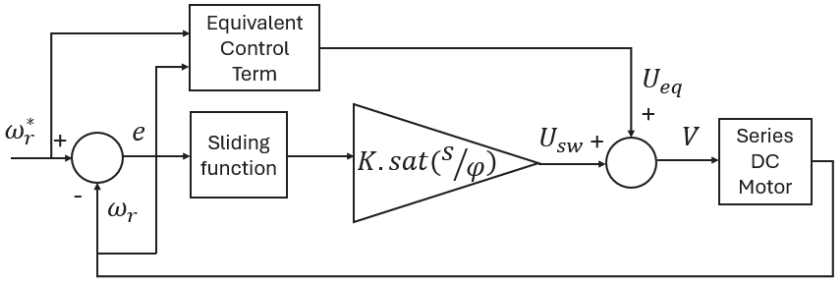

Figure 3 Block diagram of the SMC

In this study, the sliding surface is defined as given in Eq. (24).

$$s = \left(\frac{d}{dt} + \lambda\right)^{n-1} e \tag{24}$$

where n denotes the system order, and e represents the error between the desired and actual motor speeds, defined by Eq. (25).

$$e = x_1^* - x_1 \tag{25}$$

Since the series DC motor is a second-order system, n is set to 2 in Eq. (24), resulting in the sliding surface defined by Eq. (26).

$$s = \dot{e} + \lambda e \tag{26}$$

The sliding condition, which ensures the system trajectory reaches and remains on the sliding surface, is defined by Eq. (27).

$$\frac{1}{2}\frac{d}{dt}s^2 \le -\eta|s| \tag{27}$$

where η is a positive constant. By evaluating the derivative in Eq. (27), the sliding condition is reformulated as shown in Eq. (28).

$$s\dot{s} \le -\eta|s| \tag{28}$$

To ensure that the system reaches and remains on the sliding surface, the condition $\dot{s} = 0$ must be satisfied. Once the system operates on the sliding surface, robustness against external disturbances and model uncertainties is achieved. Under this condition, the derivative of the sliding surface is defined as given in Eq. (29).

$$\dot{s} = \ddot{e} + \lambda\dot{e} = \ddot{x}_1^* - \ddot{x}_1 + \lambda\dot{e} = 0 \tag{29}$$

Assuming the desired speed in the control system is constant, the second derivative $\ddot{x}_1^*$ becomes zero. Accordingly, the derivative of the sliding surface simplifies to the form given in Eq. (30).

$$\dot{s} = -\ddot{x}_1 + \lambda\dot{e} = 0 \tag{30}$$

The second-order time derivative of the angular speed $\ddot{x}_1$ for the series DC motor is expressed in Eq. (31).

$$\ddot{x}_1 = \left(\frac{2Mx_2}{J}\right)\left(\frac{V - \left(Mx_1 + R\right)x_2}{L}\right) - \frac{\dot{T}_L}{J} - \frac{b}{J}\dot{x}_1 \tag{31}$$

Since Eq. (31) contains the control variable V, which is the voltage applied for speed control of the series DC motor, the expression can be reformulated accordingly, as shown in Eq. (32).

$$\ddot{x}_1 = f + au \tag{32}$$

where u denotes the control variable, a is the coefficient associated with the control variable, and f represents the remaining terms in Eq. (31). By substituting Eq. (32) into Eq. (30), an optimal control law is derived. To ensure the satisfaction of the sliding condition, an additional discontinuous term involving the sign function is incorporated, resulting in the control variable expression given by Eq. (33).

$$u = \frac{-f + \lambda \dot{e}}{a} - k \cdot sgn(s) \tag{33}$$

The gain k must be selected sufficiently large to ensure the satisfaction of the sliding condition. The expressions for a and f, as used in Eq. (33), are presented below.

$$a = \frac{2Mx_2}{JL} \tag{34}$$

$$f = -a\left(Mx_1 + R\right)x_2 - \frac{\dot{T}_L}{J} - \frac{b}{J}\dot{x}_1 \tag{35}$$

However, incorporating a discontinuous term involving the sign function in the control variable may result in the chattering phenomenon characterized by high-frequency oscillations in the control signal. To mitigate this issue, various techniques can be employed [19]. One commonly used approach is replacing the sign function with a continuous saturation function. Under this modification, the control variable derived from the SMC is expressed as shown in Eq. (36).

$$u = \frac{-f + \lambda \dot{e}}{a} - k \cdot sat\left(s / \varphi\right) \tag{36}$$

3.3 Backstepping Sliding Mode Controller Design

Backstepping Sliding Mode Control (BSMC) is a powerful technique for regulating nonlinear systems, particularly under the influence of model uncertainties and external disturbances. In this method, the nonlinear dynamics of the series DC motor is expressed in state-space form. A speed tracking error is defined with respect to a reference speed. A sliding surface is constructed using the speed error and its derivative. This surface represents the desired closed-loop error dynamics and ensures asymptotic convergence when the system trajectory lies on it. A composite Lyapunov function, incorporating both the tracking error and the sliding surface, is formulated. Its derivative is used as a design criterion to guarantee closed-loop stability. Using the backstepping philosophy, a control law is derived such that the Lyapunov function derivative is negative semi-definite, ensuring robustness against modeling uncertainties and external disturbances. A discontinuous switching term is included to enforce the sliding condition. Fig. 4 shows the block diagram of the BSMC.

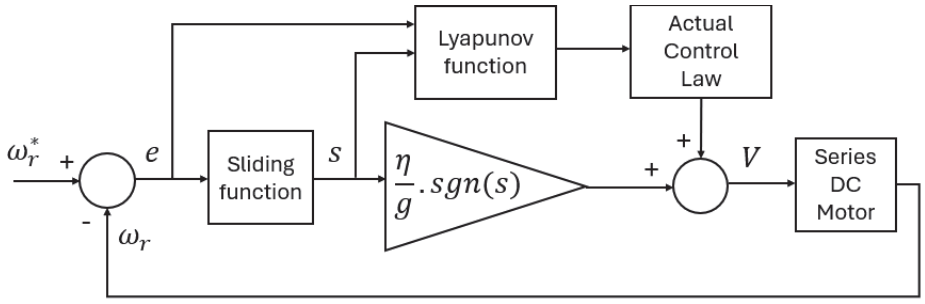

Figure 4 Block diagram of the BSMC

In this study, the nonlinear model of the series DC motor is presented below.

$$\dot{x}_1 = x_2 \tag{37}$$

$$\dot{x}_2 = f + g \cdot u + d \tag{38}$$

where x_1 denotes the motor speed, d represents the load torque acting as a disturbance input, and u is the applied DC voltage serving as the control variable. The functions f and g appearing in the system model are defined as follows.

$$f = \frac{-2L_m i^2}{J\left(L_a + L_f\right)}\left[\left(L_m\omega_r + R_f + R_a\right)\right] - \frac{1}{J}B_f\dot{\omega}_r \tag{39}$$

$$g = \frac{2L_m i}{J\left(L_a + L_f\right)} \tag{40}$$

To design the BSMC, the following steps are executed sequentially. As the first step, the speed tracking error is defined as follows:

$$e_1 = r - x_1 \tag{41}$$

where r denotes the reference value. The derivative of the speed error is given below.

$$\dot{e}_1 = \dot{r} - \dot{x}_1 = \dot{r} - x_2 \tag{42}$$

Subsequently, the sliding surface s is defined as follows:

$$s = \dot{e}_1 + c_1 e_1 \tag{43}$$

where c_1 is positive control gain. Based on Eq. (43), the derivative of the speed error is obtained as follows:

$$\dot{e}_1 = s - c_1 e_1 \tag{44}$$

To proceed with the controller design, the first Lyapunov function is defined as follows:

$$V_1 = \frac{1}{2} e_1^2 \tag{45}$$

The derivative of the Lyapunov function is expressed as follows:

$$\dot{V}_1 = e_1 \dot{e}_1 \tag{46}$$

By substituting the derivative of the speed error into Eq. (46), $\dot{V}_1$ can be reformulated as follows:

$$\dot{V}_1 = e_1 \left(\dot{r} - x_2 \right) = e_1 s - c_1 e_1^2 \tag{47}$$

By equating the expressions for $\dot{e}_1$ given in Eq. (42) and Eq. (44), the sliding surface s can be expressed as follows:

$$s = \dot{r} - x_2 + c_1 e_1 \tag{48}$$

In the second step, an extended Lyapunov function is defined as follows:

$$V_2 = V_1 + \frac{1}{2} s^2 \tag{49}$$

The derivative of the sliding surface is obtained using Eq. (48) as follows:

$$\dot{s} = \ddot{r} - \dot{x}_2 + c_1 \dot{V}_1 \dot{e}_1 \tag{50}$$

By substituting the expression for $\dot{x}_2$ from Eq. (38) into Eq. (50), $\dot{s}$ can be reformulated as follows:

$$\dot{s} = \ddot{r} - \left(f + g.u + d \right) + c_1 \dot{e}_1 \tag{51}$$

The derivative of the second Lyapunov function, as defined in Eq. (49), is given below:

$$\dot{V}_2 = \dot{V}_1 + s\dot{s} \tag{52}$$

By substituting the expressions for $\dot{V}_1$ from Eq. (47) and $\dot{s}$ from Eq. (51) into Eq. (52), $\dot{V}_2$ can be reformulated as follows:

$$\dot{V}_2 = e_1 s - c_1 e_1^2 + \ddot{s} \left[r - \left(f + g.u + d \right) + c_1 \dot{e}_1 \right] \tag{53}$$

To guarantee system stability, the condition $\dot{V}_2 \leq 0$ must be satisfied. Under this condition, the control variable derived using the BSMC is obtained as follows:

$$u = \frac{1}{g} \left(\ddot{r} - f + e_1 + c_1 \dot{e}_1 + c_2 s + \eta sgn(s) \right) \tag{54}$$

where c_2 and η are positive gains.

4 RESULTS AND DISCUSSION

When a series DC motor experiences zero torque, its speed theoretically becomes infinite. In practice, torque never fully drops to zero because mechanical friction, core losses, and stray losses are always present. Even so, operating the motor without a load can cause it to accelerate to dangerously high speeds, potentially leading to severe damage. A series motor should never be run without a load or connected through belts or similar mechanisms that could fail. If such a failure occurs during operation, the sudden loss of load could result in serious consequences. Because of the difficulties mentioned for the practical application of the series DC motor, this study was carried out in a simulation environment.

This section presents MATLAB-based simulation studies aimed at evaluating the speed control performance of a series DC motor using the proposed BSMC method. For comparative analysis, the performance of the proposed controller is benchmarked against conventional backstepping control and SMC strategies. The parameters of the series DC motor used in the simulations are provided in Tab. 1.

Table 1 Series DC motor parameters

Parameter	Value
Armature resistance (R_a)	1.5 Ω
Armature inductance (L_a)	0.12 H
Field resistance (R_f)	0.7 Ω
Field inductance (L_f)	0.03 H
Mutual inductance (L_m)	0.0675 H
Inertia torque (J)	0.02365 kg m^2
Viscous friction constant (B)	0.0025 Nms/rad

Initially, the speed control performance of the series DC motor was evaluated under a constant speed reference of 100 rad/s and a constant load torque of 5 Nm. The dynamic response of the series DC motor under these conditions is illustrated in Fig. 5.

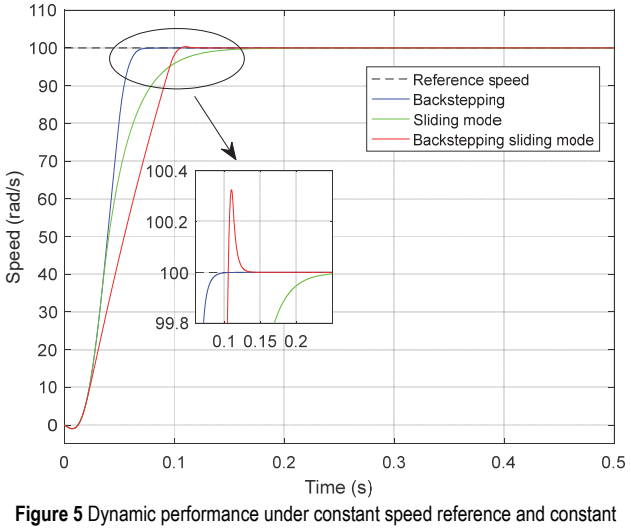

Figure 5 Dynamic performance under constant speed reference and constant load

It is observed that the backstepping controller achieves settling at the reference speed without any overshoot and in the shortest settling time of 0.1 seconds among the tested controllers. Furthermore, it demonstrates the fastest response, with a rise time of 0.031 seconds, indicating superior dynamic performance overall. The SMC also reaches the reference speed without overshoot; however, it exhibits the longest settling time of 0.21 seconds. Although the proposed BSMC shows a small overshoot of 0.32%, it settles 0.08 seconds faster than the SMC, despite having a longer rise time. Tab. 2 summarizes the dynamic performance parameters of all control methods.

Table 2 Evaluation of controllers considering transient response

Controller	Maximum overshoot / %	Rising time / s	Settling time / s
Backstepping	0	0.031	0.1
Sliding mode	0	0.056	0.21
Backstepping sliding mode	0.32	0.067	0.13

When the classical sign function is employed in the SMC, the resulting control variable is depicted in Fig. 6. In this study, the DC bus voltage is set at 200 V. As observed, the control signal rapidly switches between 0 V and 200 V, illustrating the chattering phenomenon. Such high-frequency switching in real-time implementations leads to significant switching losses.

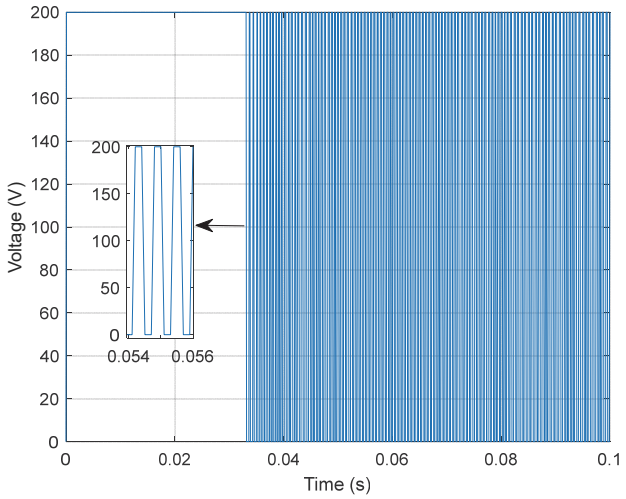

Figure 6 Control signal of the SMC using the sign function

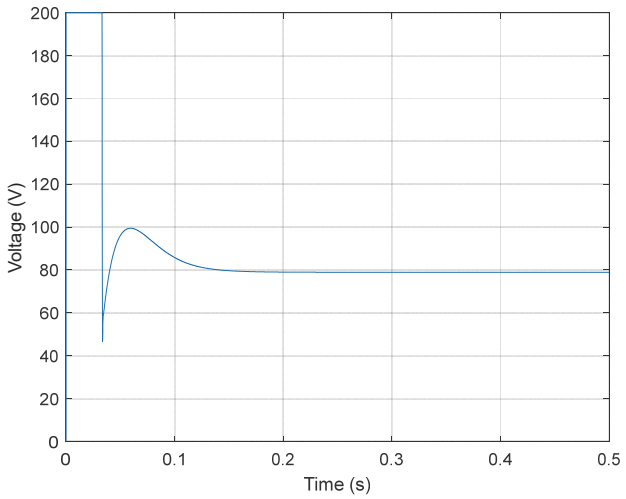

Figure 7 Control signal of the SMC using saturation function

In the SMC, a saturation function was employed to mitigate the chattering problem. The resulting control signal, illustrated in Fig. 7, demonstrates that chattering has been effectively eliminated. Additionally, the system stabilizes at the desired value with a control voltage of approximately 80 V. Therefore, if implemented in real-time, this approach would significantly reduce switching losses.

Secondly, to evaluate the speed control performance under a variable speed reference with a constant load of 5 Nm, the reference speed was stepped from 100 rad/s to 150 rad/s at t = 1.5 seconds. Fig. 8 illustrates the responses of the nonlinear controllers to this sudden change.

None of the controllers exhibited overshoot. The SMC demonstrated the longest settling time of 0.14 seconds, which is 0.05 seconds greater than those of the backstepping controller and BSMC. Among the methods tested, the BSMC provided the fastest response.

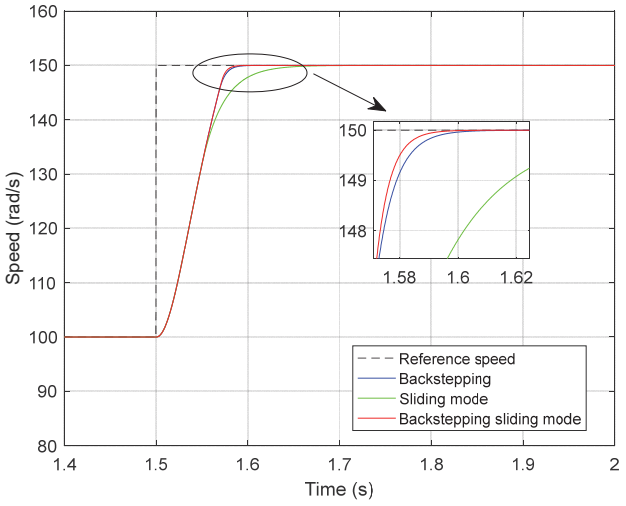

Figure 8 Dynamic performance with variable speed reference under constant load

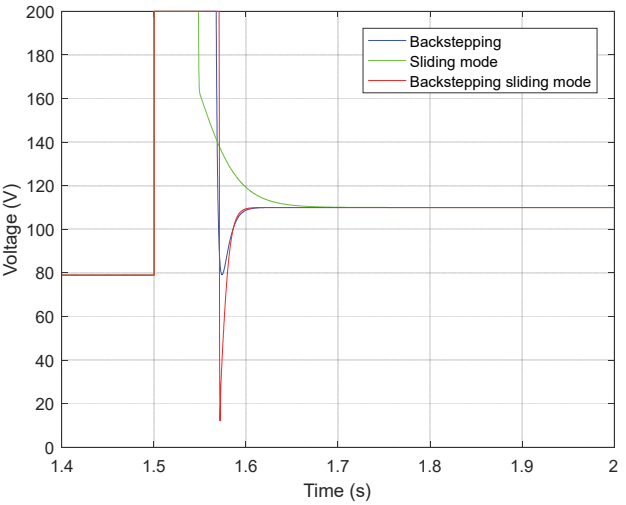

Figure 9 Variation of the control signal during sudden speed change

Fig. 9 shows the variation of the control variable over time during the speed change. As can be seen, when the speed reference suddenly increases from 100 rad/s to 150 rad/s, the armature voltage that needs to be applied to the motor increases from 80 V to 110 V.

Next, to evaluate the speed control performance under sudden load variation with a constant speed reference of 100 rad/s, the load torque was increased from 5 Nm to 10

Nm at $t = 1.5$ seconds. Fig. 10 presents the responses of the controllers to this abrupt disturbance.

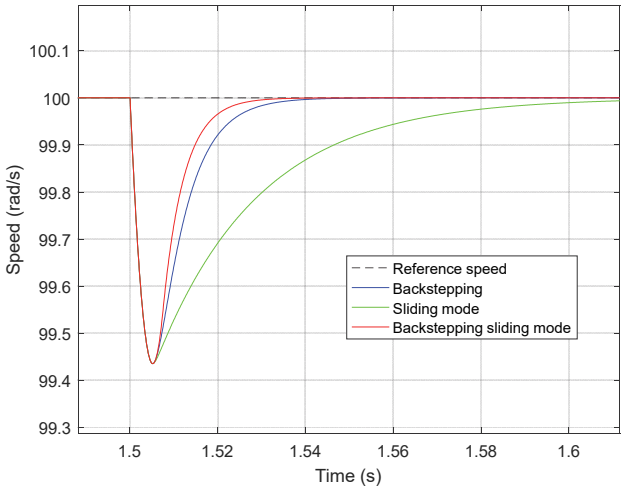

Figure 10 Dynamic performance under sudden load change

For all controllers, the sudden disturbance caused a speed drop of approximately 0.55 rad/s. However, the proposed BSMC compensated for the disturbance most rapidly, restoring the speed in 0.05 seconds. The backstepping controller followed closely, recovering in 0.06 seconds, while the SMC took 0.12 seconds. These results indicate that the proposed BSMC is the most effective in handling load variations, with the backstepping controller exhibiting comparable performance.

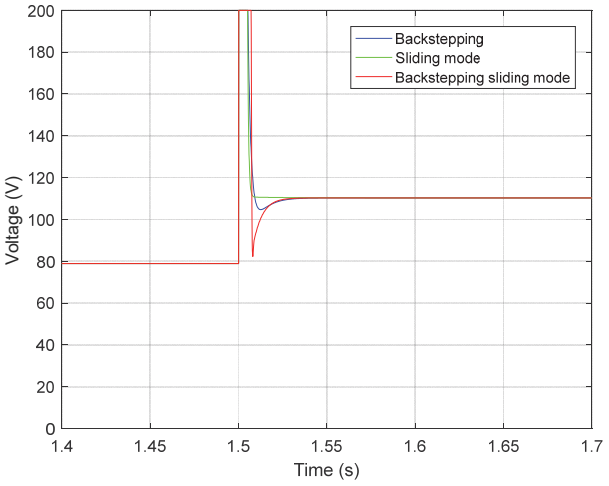

Figure 11 Variation of the control signal during sudden load change

Fig. 11 illustrates the variation in the control signal in response to the load change. As the load increased, the applied armature voltage rose from 80 V to 110 V to compensate for the speed disturbance and restore the motor speed to its reference value.

To evaluate the capability of the designed controllers for bidirectional speed control, the reference speed was set to 100 rad/s for the initial 0.5 seconds and then reversed to –100 rad/s for the subsequent 1.5 seconds. As shown in Fig. 12, all controllers successfully tracked the speed reference in both directions. During the transition to reverse operation, the backstepping controller and the proposed BSMC exhibited similar performance, while the SMC lagged by 0.25 seconds and exhibited a 21% overshoot.

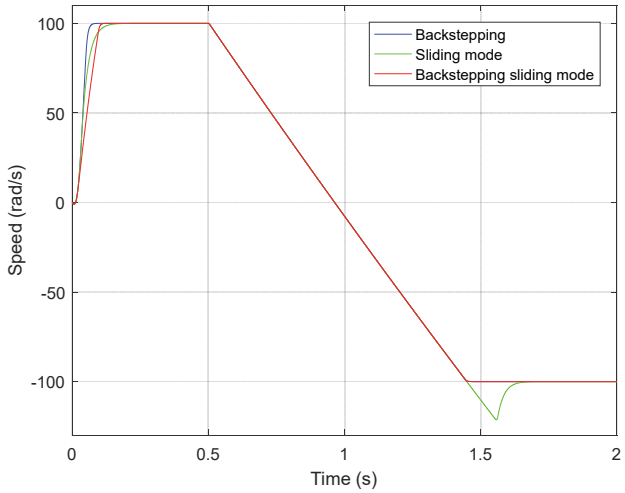

Figure 12 Dynamic response during bidirectional operation

Finally, the speed control performance of the series DC motor was evaluated under ±50% parameter uncertainty. For this test, the system operated under a reference speed of 100 rad/s and a load torque of 5 Nm until 3 seconds. At $t = 3$ s, the reference speed was increased to 150 rad/s, and at $t = 6$ s, the load torque was increased to 10 Nm. Fig. 13 illustrates the dynamic response of the motor under +50% parameter uncertainty, while Fig. 14 presents the corresponding variation in the control signal.

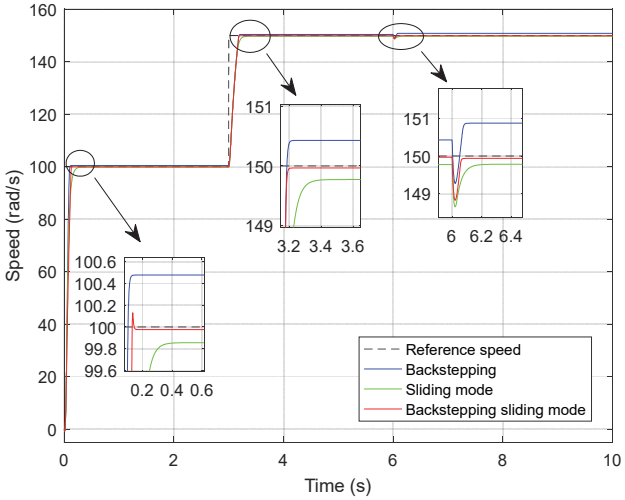

Figure 13 Dynamic performance under +50% parameter uncertainty

As observed in Fig. 13, during the interval up to the 3rd second, when both the speed reference and load torque remain constant, the highest steady-state error occurs with the backstepping controller, reaching 0.47 rad/s. The SMC performs better, with a steady-state error of 0.15 rad/s. The proposed BSMC achieves the most accurate tracking, exhibiting the lowest steady-state error of just 0.02 rad/s.

Between the 3rd and 6th seconds, following the increase in the reference speed, the highest steady-state error is again observed with the backstepping controller at 0.42 rad/s. The SMC exhibits a reduced steady-state error of 0.23 rad/s. Consistent with earlier results, the proposed BSMC delivers the best performance, maintaining an almost negligible steady-state error of 0.03 rad/s.

Following the sudden load change at the 6th second, the backstepping controller exhibits the highest steady-state error of 0.87 rad/s. The SMC performs comparatively

better, with a steady-state error of 0.22 rad/s. Once again, the proposed BSMC demonstrates superior performance, achieving the lowest steady-state error of just 0.06 rad/s.

Based on these results, the BSMC demonstrates the highest robustness against +50% parameter uncertainty, while the backstepping controller is the least effective. Furthermore, the findings indicate that increased load torque leads to a corresponding increase in steady-state error across all controllers.

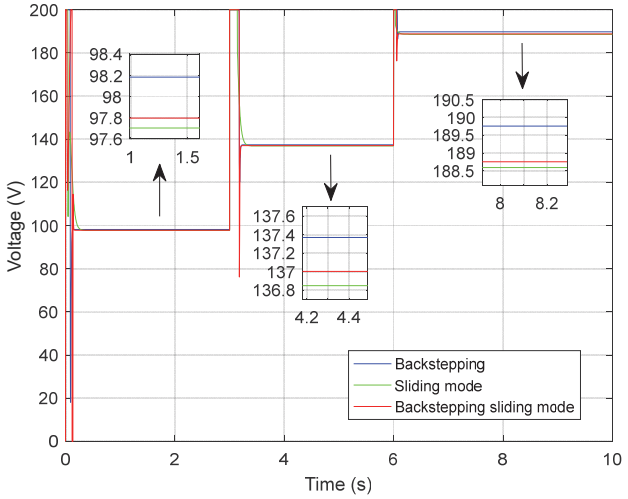

Figure 14 Variation of the control signal under +50% parameter uncertainty

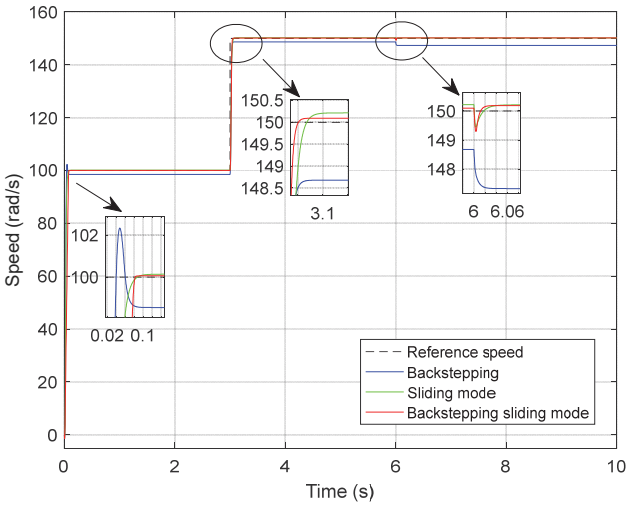

Figure 15 Dynamic performance under –50% parameter uncertainty

Fig. 15 presents the dynamic performance of the series DC motor under −50% parameter uncertainty, while Fig. 16 illustrates the corresponding variation of the control signal. Upon examining Fig. 15, it is observed that before the 3rd second, the backstepping controller exhibits the highest steady-state error at 1.46 rad/s. The SMC performs better in comparison, with a steady-state error of 0.14 rad/s. The proposed BSMC demonstrates the best performance, achieving the lowest steady-state error of 0.06 rad/s.

Between the 3rd and 6th seconds, the backstepping controller continues to exhibit the highest steady-state error, measured at 1.33 rad/s. In contrast, the SMC achieves a significantly lower error of 0.22 rad/s. The proposed BSMC again demonstrates superior performance, maintaining a low steady-state error of 0.09 rad/s.

After the 6th second, the backstepping controller once again exhibits the highest steady-state error, reaching 2.67 rad/s. The proposed BSMC maintains its superior performance with the lowest error of 0.18 rad/s. The SMC also shows comparable effectiveness, with a steady-state error of 0.21 rad/s.

These results indicate that, as with the +50% parameter uncertainty case, the most robust controller against –50% parameter uncertainty is the proposed BSMC, while the least effective is the backstepping controller. Moreover, while increasing the load leads to an increase in steady-state errors for most controllers, the SMC maintains a nearly constant error, demonstrating its robustness to load variations.

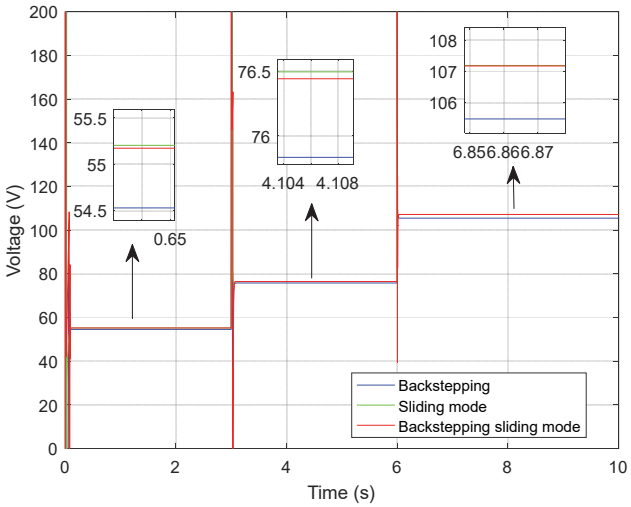

Figure 16 Variation of the control signal under –50% parameter uncertainty

The robustness performance of the controllers under ±50% parameter uncertainty is quantitatively summarized using the Integral of Absolute Error (IAE), as presented in Tab. 3. Under +50% parameter uncertainty, the proposed BSMC achieves the lowest IAE value of 11.6296, indicating the most accurate overall tracking performance. The SMC follows with an IAE of 13.1155, while the backstepping controller records the highest IAE of 15.8843. These results confirm the superior robustness of the BSMC in the presence of increased system parameters, which is consistent with the time-domain responses shown in Fig. 13. The relatively higher IAE of the backstepping controller reflects its increased steady-state errors and sensitivity to parameter variations.

Table 3 IAE values for robustness performance of the controllers

Controller	IAE values	
	+50% parameter uncertainty	–50% parameter uncertainty
BSMC	11.6296	6.4668
SMC	13.1155	5.5408
Backstepping	15.8843	22.2263

Under −50% parameter uncertainty, the BSMC and SMC exhibit comparable robustness, with IAE values of 6.4668 and 5.5408, respectively. As can be understood from Fig. 15, although the BSMC exhibits a lower steady-state error compared to the SMC, a lower IAE value is obtained with the SMC due to its slightly shorter rise time in transient performance. In contrast, the backstepping controller demonstrates significantly degraded

performance, with a much larger IAE of 22.2263, confirming its limited robustness to parameter reductions. This behaviour aligns with the large steady-state errors observed in Fig. 15.

5 CONCLUSIONS

This paper presented a BSMC for robust speed control of a series DC motor with strongly nonlinear dynamics. By integrating the recursive stabilization framework of backstepping with the robustness properties of SMC, the proposed approach achieves stable and accurate speed regulation in the presence of load disturbances and significant parameter uncertainties. Lyapunov-based analysis guarantees closed-loop stability, while simulations validate the controller's effectiveness under a wide range of operating conditions.

The comparative study highlights the complementary strengths of the individual control strategies. While the backstepping controller performs well when motor parameters are precisely known, its performance degrades under uncertainty. SMC improves robustness but suffers from slower transient response. The proposed BSMC successfully combines the advantages of both methods, delivering improved robustness, fast disturbance rejection, and accurate tracking without sacrificing stability, thereby providing a more reliable solution for series DC motor speed control.

Although BSMC offers superior robustness and tracking performance compared with SMC and conventional backstepping, its enhanced control capability is achieved at the cost of increased computational complexity.

From a structural perspective, SMC typically requires computation of a sliding surface and a discontinuous control law, resulting in relatively low online computational demand. Similarly, classical Backstepping involves recursive Lyapunov-based controller synthesis, which is more computationally intensive than SMC. In contrast, BSMC integrates the recursive design of backstepping with the nonlinear switching mechanism of SMC, leading to a layered control structure that increases both symbolic complexity during design and numerical burden during online execution.

Despite this increased complexity, it is important to note that modern digital signal processors (DSPs), field-programmable gate arrays (FPGAs), and high-performance microcontrollers significantly alleviate these concerns. For this application, the computational overhead of BSMC remains within acceptable limits, particularly when the control algorithm is efficiently implemented and unnecessary symbolic redundancy is eliminated.

Future research will focus on experimental validation of the proposed controller on a real-time test bench, as well as the development of reduced-complexity or adaptive versions of BSMC to further lower computational requirements.

6 REFERENCES

[1] Roy, T. K., Morshed, M., Tumpa, F. K., & Pervej, M. F. (2015). Robust adaptive backstepping speed controller design for a series DC motor. *2015 IEEE International WIE Conference on Electrical and Computer Engineering (WIECON-ECE)*, 243-246. https://doi.org/10.1109/WIECON-ECE.2015.7443908

[2] Hozefa, J., Ankit, M., Shadab, S., & Bhil, S. K. (2020). Feedback linearization technique for DC series motor with LMI based observer and DREM. *Proceedings of the International Conference on Smart Grids and Energy Systems (SGES)*, 407-412. https://doi.org/10.1109/SGES51519.2020.00078

[3] Duan, Q., & Zhang, Y. (2020). Analysis and implementation of series excitation DC motor control system. *Proceedings of the IEEE 9th Joint International Information Technology and Artificial Intelligence Conference (ITAIC)*, 144-147. https://doi.org/10.1109/ITAIC49862.2020.9338887

[4] Bitar, Z., Al Jabi, S., & Khamis, I. (2014). Modeling and simulation of series DC motors in electric car. *Energy Procedia*, *50*, 460-470. https://doi.org/10.1016/j.egypro.2014.06.056

[5] Ihor, O., Larysa, A., & Serhii, B. (2021). Research of closed loop control systems of the electric drive of mine electric locomotive with the DC series motor and nonlinear load. *Proceedings of the IEEE International Conference on Modern Electrical and Energy Systems (MEES)*, 1-6. https://doi.org/10.1109/MEES52427.2021.9598735

[6] Liceaga-Castro, J. U., Siller-Alcalá, I. I., Jaimes-Ponce, J., Alcántara-Ramírez, R. A., & Zamudio, E. A. (2017). Identification and real-time speed control of a series DC motor. *Mathematical Problems in Engineering*, *2017*(1), 7348263. https://doi.org/10.1155/2017/7348263

[7] Muruganandam, M. & Madheswaran, M. (2012). Experimental verification of chopper fed DC series motor with ANN controller. *Frontiers in Electrical and Electronic Engineering*, *7*(4), 477-489. https://doi.org/10.1007/s11460-012-0211-1

[8] Madhusudhana Rao, G. & Sanker Ram, B. V. (2009). Speed control of multilevel inverter designed DC series motor with neuro-fuzzy controllers. *Journal of Computing*, *1*(1), 179-186.

[9] Tushir, M. & Srivastava, S. (2011). Type-2 fuzzy logic controller implementation for tracking control of DC motor. *International Journal of Computer Network and Security*, *3*(1), 34-41.

[10] Farooq, U., Gu, J., Asad, M. U., & Abbas, G. (2014). Robust Takagi-Sugeno fuzzy speed regulator for DC series motors. *Proceedings of the 12th International Conference on Frontiers of Information Technology*, 79-86. https://doi.org/10.1109/FIT.2014.24

[11] Lee, Y.-C., Lin, Y.-H., Chang, W.-J., Aslam, M. S., & Lin, Z.-Y. (2025). Optimal fuzzy tracking synthesis for nonlinear discrete-time descriptor systems with T-S fuzzy modeling approach. *CMES - Computer Modeling in Engineering & Sciences*, *143*(2), 1433-1461. https://doi.org/10.32604/cmes.2025.064717

[12] Visavakitcharoen, A., Assawinchaichote, W., Shi, Y., & Angeli, C. (2023). Event-triggered fuzzy integral control for a class of nonlinear singularly perturbed systems. *ISA Transactions*, *139*, 71-85. https://doi.org/10.1016/j.isatra.2023.04.011

[13] Abdullah, A. & Qasem, O. (2019). Full-order and reduced-order observers for linear parameter-varying systems with one-sided Lipschitz nonlinearities and disturbances using parameter-dependent Lyapunov function. *Journal of the Franklin Institute*, *356*(10), 5541-5572. https://doi.org/10.1016/j.jfranklin.2019.04.029

[14] Bisoi, A., Samantaray, A. K., & Bhattacharyya, R. (2017). Control strategies for DC motors driving rotor dynamic systems through resonance. *Journal of Sound and Vibration*, *411*, 304-327. https://doi.org/10.1016/j.jsv.2017.09.014

[15] Traue, G., Book, W., Kirchgässner, F., & Wallscheid, O. (2022). Toward a reinforcement learning environment

toolbox for intelligent electric motor control. *IEEE Transactions on Neural Networks and Learning Systems*, *33*(3), 919-928. https://doi.org/10.1109/TNNLS.2020.3029573

[16] Rodríguez-Abreo, O., Aviles, M., Rodríguez-Reséndiz, J., & García-Cerezo, A. (2025). Neural networks and genetic algorithms-based self-adjustment system for a backstepping controller of an unmanned aerial vehicle. *Alexandria Engineering Journal*, *126*, 70-80. https://doi.org/10.1016/j.aej.2025.04.034

[17] Srief, M. L., Soltane, B., Lokmane, N. A., & Malak, G. (2024). A complete control structure based backstepping controller design for stacked multi-cell multi-level SPWM VSC STATCOM. *Energy Reports*, *12*, 687-698. https://doi.org/10.1016/j.egyr.2024.06.051

[18] Hua, L.-G., Ali, A., Ullah, S., Hafeez, G., Zaidi, M. M., & Jun, L. J. (2023). Robust finite-time integral terminal sliding mode control design for maximum power extraction of PMSG-based standalone wind energy system. *Frontiers in Energy Research*, *11*, 1293267. https://doi.org/10.3389/fenrg.2023.1293267

[19] Ullah, A., Ullah, S., Zhang, Z., & Jianfei, P. (2025). Smooth super-twisting sliding mode control design with high order super-twisting observer for speed tracking control of permanent magnet synchronous motor drive system. *ISA Transactions*, *162*, 227-242. https://doi.org/10.1016/j.isatra.2025.04.007

Contact information:

Hamed Khaled SHREITEH
Department of Mechatronics Engineering,
Karabuk University,
78050, Merkez, Karabük, Turkey
E-mail: hamed.shreteih@gmail.com

Hilmi AYGÜN, Assistant Professor
(Corresponding author)
Department of Mechatronics Engineering,
Karabuk University,
78050, Merkez, Karabük, Turkey
E-mail: hilmiaygun@karabuk.edu.tr